Many-body physics of Rydberg dark-state polaritons in the strongly interacting regime

Matthias Moos,* Michael Höning, Razmik Unanyan, and Michael Fleischhauer
Fachbereich Physik und Forschungszentrum OPTIMAS, Technische Universität Kaiserslautern, 67663 Kaiserslautern, Germany
(Received 29 June 2015; revised manuscript received 30 September 2015; published 19 November 2015)

Coupling light to Rydberg states of atoms under conditions of electromagnetically induced transparency (EIT) leads to the formation of interacting quasiparticles, termed Rydberg polaritons. We derive a one-dimensional model describing the time evolution of these polaritons under paraxial propagation conditions. Specifically, we obtain a master equation governing the dynamics of Rydberg polaritons and identify conditions when it can essentially be described by an effective Hamiltonian of a single-species polariton. We verify this Hamiltonian by numerical two-excitation simulations. Under typical stationary EIT conditions it is impossible to reach the strongly interacting regime where long-range density-density correlations emerge. In contrast, by employing the time dependence of the control field the regime of strong interactions can be reached where the polaritons attain quasicrystalline order. We provide a physical explanation for the differences between stationary and time-dependent schemes.

DOI: 10.1103/PhysRevA.92.053846 PACS number(s): 42.50.Nn, 32.80.Ee, 32.80.Qk, 42.50.Gy

I. INTRODUCTION

There has been growing interest in using Rydberg gases [1] to tailor strong and nonlocal nonlinearities for photons. The strong interactions between Rydberg states in a gas of ultracold atoms can mediate strong nonlocal interactions for light fields propagating under conditions of electromagnetically induced transparency (EIT) in such a medium [2–10]. For instance, the formation of a small blockaded volume leading to antibunching of photons as well as pronounced bunching of photons in a Rydberg gas has been demonstrated experimentally [11,12]. Moreover, first steps have been taken towards building single-photon logic devices using Rydberg gases, such as single-photon switches [13–16].

Their pronounced interaction makes Rydberg polaritons interesting candidates to study many-body effects in the strongly correlated regime, where the interaction energy dominates the kinetic energy. In the present paper we consider the propagation of light in Rydberg EIT media under paraxial conditions with transversal confinement, as can be realized experimentally, e.g., using cigar-shaped atomic ensembles or sending photons through hollow-core optical fibers filled with Rydberg atoms [17,18]. In a previous Letter [19] we argued that the propagation of photons inside Rydberg gases under EIT conditions can be described in terms of interacting quasiparticles, named Rydberg polaritons. Assuming that the polaritons are at all times close to the ground state of an effective one-dimensional model and using a Luttinger-liquid approximation, we showed that a regime of strong correlations can be reached by dynamically turning photons into stationary Rydberg excitations [20].

In the present paper we extend these studies by deriving the effective dark-state polariton model including leading-order corrections valid for sufficiently large separation of Rydberg polaritons. This regime allows for a perturbative treatment of the coupling between bright- and dark-state polaritons. We obtain a Lindblad master equation for the Rydberg dark-state polaritons where the bright-state polaritons act as a Markovian reservoir. We verify the model by employing numerical two-excitation wave-function simulations. We derive conditions when the master equation can be reduced to the effective Hamiltonian introduced in [19]. Furthermore, we show that for an excitation density smaller than one per blockade volume and a transversal beam diameter less than the blockade radius the paraxial propagation can be described by a one-dimensional model. The wave-function simulations show that injecting an initial photon wave packet into a Rydberg EIT medium and subsequent storage leads to a quantum state close to the ground state of the effective Hamiltonian. Finally we provide a simple physical picture why reaching the strongly interacting regime under cw conditions is impossible in typical EIT systems and how a dynamical storage sequence can circumvent this problem.

The paper is organized as follows. In Sec. II we introduce the microscopic model of photons coupled to interacting three-level atoms and derive conditions when the free as well as the interacting problem reduces to a one-dimensional model. In Sec. III we derive a Born-Markovian master equation for the dark-state polaritons by treating the bright-state polaritons as a reservoir and discuss corrections to the simple unitary time evolution introduced in [19]. In Sec. IV we employ numerical two-excitation wave-function simulations to verify the model and analyze the quantum state after sending a light pulse into a Rydberg gas under EIT conditions. Finally, in Sec. V we discuss many-body properties of the interacting problem and point out the differences between stationary EIT and a light storage scheme.

II. RYDBERG POLARITONS

In this section we discuss the paraxial propagation of weak light pulses in an atomic medium under EIT conditions with Rydberg interactions. We introduce our model and derive conditions for the reduction of the full interaction problem to a one-dimensional model with an effective Hamiltonian.

A. Light-matter coupling

Let us consider a system of a weak quantized probe field $\hat{E} = \sqrt{\frac{\hbar\omega_p}{2\epsilon_0}}\hat{\mathcal{E}}e^{-i(\omega_p t - k_p z)} + \text{H.a.}$ propagating through an ensemble of three-level atoms as sketched in Fig. 1(b)

*mmoos@physik.uni-kl.de

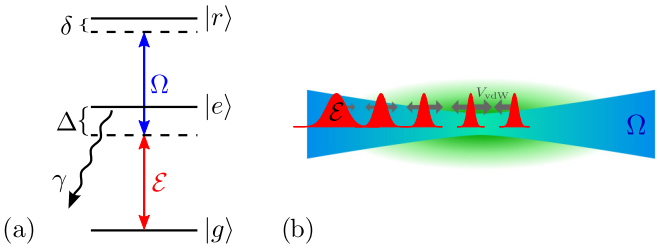

FIG. 1. (Color online) (a) Atomic level scheme with input probe field $\mathcal{E}$ and control field Ω. (b) Sketch of a possible experimental realization: one-dimensional setup with copropagating photons focused inside an atomic cloud of Rydberg atoms and control field Ω.

with the level structure in a ladder configuration as in [21] and as drawn in Fig. 1(a). The operators $\hat{\mathcal{E}},\hat{\mathcal{E}}^\dagger$ are slowly varying envelope operators, which obey bosonic commutation relations $[\hat{\mathcal{E}}(\mathbf{r}),\hat{\mathcal{E}}^\dagger(\mathbf{r}')] = \delta(\mathbf{r}-\mathbf{r}')$. Here ω_p and k_p denote the carrier frequency and wave number of the probe field, respectively. The atoms are composed of a ground state $|g\rangle$, an intermediate excited state $|e\rangle$, and a metastable Rydberg state $|r\rangle$. We neglect dipole-dipole interactions of Rydberg states for a moment, which we will reintroduce later. The field $\hat{\mathcal{E}}$ couples the atomic states $|g\rangle$ and $|e\rangle$ with single-photon detuning $\Delta = \omega_{eg} - \omega_\mathrm{p}$, where $\omega_{\mu\nu} = (E_\mu - E_\nu)/\hbar$ denotes the transition frequency between atomic states $|\mu\rangle$ and $|\nu\rangle$. The transition between states $|e\rangle$ and $|r\rangle$ is driven by a classical control field Ω with carrier frequency ω_c and detuning $\Delta_\mathrm{c} = \omega_{re} - \omega_\mathrm{c}$. We denote the resulting two-photon detuning by $\delta = \Delta + \Delta_\mathrm{c}$. The atomic state $|e\rangle$ is assumed to be subject to spontaneous decay with rate γ.

The polarization and the spin coherence are microscopically described by spin flip operators $|\mu\rangle\langle\nu|$ of individual atoms. By averaging these over a small volume centered at a position $\mathbf{r}$ and containing $N_\mathbf{r} \gg 1$ atoms we define continuous, coarse-grained atomic operators $\sigma_{\mu\nu}$ at position $\mathbf{r}$,

$$\hat{\sigma}_{\mu\nu}(\mathbf{r}) = \frac{1}{N_\mathbf{r}} \sum_{j=1}^{N_\mathbf{r}} |\mu\rangle_{jj}\langle\nu|, \tag{1}$$

which fulfill the commutation relations $[\hat{\sigma}_{\alpha\beta}(\mathbf{r}),\hat{\sigma}_{\mu\nu}(\mathbf{r}')] = \frac{1}{n}\delta(\mathbf{r}-\mathbf{r}')[\delta_{\beta\mu}\hat{\sigma}_{\alpha\nu}(\mathbf{r}) - \delta_{\alpha\nu}\hat{\sigma}_{\mu\beta}(\mathbf{r})]$, where we assume the density n of the atoms to be homogeneous. Transforming to a frame rotating with the atomic frequencies and performing the rotating-wave approximation, the atom-light coupling Hamiltonian of this system can be written as ($\hbar = 1$)

$$\begin{aligned}\hat{H} = n \int d^3\mathbf{r}\{&\Delta\hat{\sigma}_{ee}(\mathbf{r}) + \delta\hat{\sigma}_{rr}(\mathbf{r})\} \\ &- \{\Omega\hat{\sigma}_{re}(\mathbf{r}) + g\sqrt{n}\hat{\mathcal{E}}(\mathbf{r})\hat{\sigma}_{eg}(\mathbf{r}) + \text{H.a.}\},\end{aligned} \tag{2}$$

where $g = d_{ge}\sqrt{\omega_{ge}/2\hbar\epsilon_0}$ denotes the coupling strength of the electric field $\hat{\mathcal{E}}$ to the atomic transition $|g\rangle - |e\rangle$, with d_{ge} being the corresponding dipole matrix element.

We derive Heisenberg-Langevin equations of motion for the slowly varying field $\hat{\mathcal{E}}$ and coarse-grained atomic operators taking into account the spontaneous decay rate γ of the intermediate level [22]. Assuming the probe field to be weak compared to the control field, we can treat the equations in linear response with respect to $g\hat{\mathcal{E}}$, leading to the equations of motion for the polarization $\hat{\sigma}_{ge}$ and spin coherence $\hat{\sigma}_{gr}$,

$$\begin{aligned}\partial_t\hat{\sigma}_{gr} &= -i\delta\hat{\sigma}_{gr} + i\Omega\hat{\sigma}_{ge} \\ \partial_t\hat{\sigma}_{ge} &= -\Gamma\hat{\sigma}_{ge} + ig\sqrt{n}\hat{\mathcal{E}} + i\Omega\hat{\sigma}_{gr} + \hat{F}_{ge},\end{aligned} \tag{3}$$

where $\Gamma = \gamma + i\Delta$ and $\hat{F}_{ge}$ denotes a Langevin noise operator [22], which is δ correlated in time and space with a vanishing expectation value that needs to be added to preserve the commutation relations. As the noise is related to the population of the excited state, which we set as $\hat{\sigma}_{ee} = 0$ in linear response, the Langevin operators can be neglected. In the following we consider only the case of two-photon resonant driving, i.e., $\delta = 0$.

B. Paraxial light propagation

The dynamics of the probe field is described by the truncated paraxial wave equation

$$\left(\partial_t + c\partial_z - i\frac{c}{2k_p}\nabla_\perp^2\right)\hat{\mathcal{E}}(\mathbf{r},t) = ig\sqrt{n}\hat{\sigma}_{ge}(\mathbf{r},t). \tag{4}$$

We assume a cylindrical symmetry of the experimental setup and decompose the probe field into mode functions $u_{\mu\nu}(r,\varphi)$, which are eigensolutions of $\nabla_\perp^2 u_{\mu\nu}(r,\varphi) = 0$,

$$\hat{\mathcal{E}}(\mathbf{r},t) = \sum_{\mu,\nu} u_{\mu\nu}(r,\varphi)\hat{\mathcal{E}}_{\mu\nu}(z,t). \tag{5}$$

The mode functions

$$u_{\mu\nu}(r,\varphi) = \frac{C_{\mu\nu}}{w_0}\left[\frac{\sqrt{2}r}{w_0}\right]^{|\mu|} e^{-r^2/w_0^2 + i\mu\varphi} L_\nu^{|\mu|}\left(\frac{2r^2}{w_0^2}\right) \tag{6}$$

are a complete orthogonal set in the cylindrical coordinates (r,ϕ). Here L_ν^μ are the associated Laguerre polynomials, $C_{\mu\nu}$ are appropriate normalization constants, and ν and μ denote the radial and azimuthal indices of the mode functions, respectively. Replacing $w_0 \to w(z)$, Eq. (5) describes Gauss-Laguerre modes of paraxial light propagation [23]. For z values well within the Rayleigh length $z_R = \pi w_0^2/\lambda_p$, one finds $w(z) \approx w_0 = \text{const}$ and (5) becomes an adequate decomposition.

We decompose $\hat{\sigma}_{ge}(\mathbf{r},t)$ and $\hat{\sigma}_{gr}(\mathbf{r},t)$ into the modes $u_{\mu\nu}(r,\varphi)$ in an analogous way and obtain from Eq. (4) and the completeness relation of the mode functions

$$\begin{aligned}&(\partial_t + c\partial_z)\hat{\mathcal{E}}_{\mu\nu}(z,t) \\ &\quad = ig\sum_{\alpha,\beta}\int dr\, d\varphi\sqrt{n(\mathbf{r})}u_{\mu\nu}^*(r,\varphi)u_{\alpha\beta}(r,\varphi)\hat{\sigma}_{ge}^{\alpha\beta}(z,t).\end{aligned} \tag{7}$$

If the atomic density $n(\mathbf{r})$ is slowly varying spatially in r on the scale w_0 and is furthermore independent of φ, orthogonality of the modes yields

$$(\partial_t + c\partial_z)\hat{\mathcal{E}}_{\mu\nu}(z,t) = ig\sqrt{n}\hat{\sigma}_{ge}^{\mu\nu}(z,t). \tag{8}$$

If also the driving-field Rabi frequency is independent of φ and slowly varying in r, the Heisenberg-Langevin equations (3) decouple in the transverse modes $u_{\mu\nu}(r,\varphi)$ as well. In this case, the equations of motion can be reduced to a one-dimensional propagation problem for the individual transverse modes. Note that this is only correct as long as interactions are disregarded. The effect of the latter will be discussed later on.

In the following we drop the index (0,0) since we are interested in particular in the Gaussian input mode $\hat{\mathcal{E}}_{0,0}$.

C. Slow-light polaritons

Assuming that the control field $\Omega(z,t)$ is slowly varying in z on the scale w_0 yields a system of linear partial differential equations for the probe field and the atomic operators, which separate in the transverse modes. Restricting to the lowest transverse mode and defining $\mathbf{x} = (\hat{\mathcal{E}},\hat{\sigma}_{gr},\hat{\sigma}_{ge})^T$, we can write equations of motion for $\mathbf{x}$ as

$$i\partial_t \mathbf{x} = H\mathbf{x}, \quad H = \begin{pmatrix} -ic\partial_z & 0 & -g\sqrt{n} \\ 0 & 0 & -\Omega \\ -g\sqrt{n} & -\Omega & -i\Gamma \end{pmatrix}, \tag{9}$$

termed the Maxwell-Bloch equations. In Fourier space we find the momentum eigenmodes of these equations. The small momentum ($k \approx 0$) eigenmodes are the so-called dark-state polariton mode and two corresponding bright-state polariton modes [21]. The dark-state polariton is a superposition of electric field and spin coherence $\hat{\sigma}_{gr}$: $\hat{\Psi} = \cos\theta\hat{\mathcal{E}} - \sin\theta\sqrt{n}\hat{\sigma}_{gr}$, where the mixing angle θ is given by $\tan^2\theta = g^2n/\Omega^2$. We define the bright-state polariton as $\hat{\Phi} = \sin\theta\hat{\mathcal{E}} + \cos\theta\sqrt{n}\hat{\sigma}_{gr}$, which is not an eigenmode of (9), but is a more convenient definition. Assuming the complex decay rate Γ to define the shortest time scale as $|\Gamma|^{-1}$, the $\hat{\sigma}_{ge}$ can be adiabatically eliminated. Transforming the remaining fields $\hat{\mathcal{E}},\hat{\sigma}_{gr}$ to the polariton basis $\mathbf{y} = (\hat{\Psi},\hat{\Phi})^T$ leads to the equations of motion

$$i\partial_t \mathbf{y} = H'\mathbf{y}, \quad H' = \begin{pmatrix} c\cos^2\theta\partial_z & c\sin\theta\cos\theta\partial_z \\ c\sin\theta\cos\theta\partial_z & c\sin^2\theta\partial_z + \Gamma_{\text{eff}} \end{pmatrix}. \tag{10}$$

Here we defined the effective decay rate of the bright-state polaritons as $\Gamma_{\text{eff}} = \Omega_e^2/\Gamma$, with $\Omega_e^2 = g^2n + \Omega^2$. Comparing the off-diagonal coupling between dark- and bright-state polaritons to the difference of the diagonal terms, we find that we can treat the off-diagonal terms perturbatively if

$$c|k| \ll |\Gamma_{\text{eff}}| \tag{11}$$

is fulfilled for all relevant k values of the polariton field. In this case one recognizes directly from Eq. (10) that $\hat{\Psi}$ is a stationary dark state propagating lossless with reduced group velocity $v_g = c\cos^2\theta \ll c$ (slow light). We note that condition (11) sets a limit for the characteristic length scale of the dark-state polaritons

$$l_{\text{DSP}} \gg \frac{c|\Gamma|}{\Omega_e^2} \approx \frac{|\Delta|}{\gamma} L_{\text{abs}}, \tag{12}$$

where the approximation holds in the off-resonance case and $L_{\text{abs}} = c\gamma/g^2n$ denotes the resonant absorption length of the medium. It is immediately clear that many-body effects can only be observed when many excitations fit inside the medium, i.e., $l_{\text{DSP}} \ll L$, with L being the medium length, requiring media with large optical depth $d = L/L_{\text{abs}} \gg 1$.

D. Rydberg interactions

For highly excited Rydberg states $|r\rangle$, dipole-dipole interactions between atoms become important, due to their large dipole moments [24]. Atoms in a state $|r\rangle$ interact with the van der Waals interaction potential $V(r) = C_6/|r|^6$ with interaction strength C_6. For an ensemble of Rydberg atoms the microscopic Hamiltonian describing the interaction reads

$$\hat{V} = \frac{1}{2}\sum_{i,j\neq i} \hat{\sigma}_{rr}^{(i)} V(\mathbf{r}_i - \mathbf{r}_j)\hat{\sigma}_{rr}^{(j)}, \tag{13}$$

where $\hat{\sigma}_{rr}^{(i)}$ denotes the projection operator to the Rydberg state of atom i at position $\mathbf{r}_i$. Assuming a small excitation probability per atom to the Rydberg state allows us to set $\hat{\sigma}_{rr} \approx \hat{\sigma}_{gr}^\dagger\hat{\sigma}_{gr}$ by means of a Holstein-Primakoff transformation. Transforming to coarse-grained operators according to Eq. (1) and performing the continuum limit as above finally leads to the continuous interaction Hamiltonian

$$\hat{H}_{\text{int}} = \frac{n^2}{2}\int d^3\mathbf{r}\int d^3\mathbf{r}' V(\mathbf{r}-\mathbf{r}')\hat{\sigma}_{gr}^\dagger(\mathbf{r})\hat{\sigma}_{gr}^\dagger(\mathbf{r}')\hat{\sigma}_{gr}(\mathbf{r}')\hat{\sigma}_{gr}(\mathbf{r}). \tag{14}$$

This interaction between Rydberg excitations gives rise to a two-photon level shift, which exceeds the EIT linewidth (11) when the distance between two excitations becomes less than the EIT blockade radius

$$a_{\text{B}} = \sqrt[6]{|C_6\Gamma|/\Omega^2}. \tag{15}$$

For short distances the mixing between dark- and bright-state polaritons becomes strong and leads to a suppression of multiple excitations, which is the so-called Rydberg blockade [25]. Here the polariton picture is no longer adequate [26,27]. However, if the excitation density is smaller than a_{B}^{-3} the polariton picture is expected to hold true. It should be noted that under slow-light conditions Ω^2 becomes small and accordingly the blockade radius a_{B} becomes large. In the limit of light storage, where $\Omega(t) \to 0$, one finds $a_{\text{B}} \to \infty$ and thus it is unclear if light storage in a Rydberg EIT medium is possible at all. We will show below, however, that the critical distance between excitations at which a significant mixing between polaritons sets in is *not* given by a_{B} but instead by

$$a_{\text{c}} = \sqrt[6]{|C_6\Gamma|/\Omega_e^2}, \tag{16}$$

which stays finite in the limit of light storage, as $\Omega_e^2 \to g^2n$.

E. Reduction to a one-dimensional model

While the paraxial light propagation in a linear EIT medium can be described by a one-dimensional model, this no longer holds in general true if there are interactions between polaritons. The Rydberg interactions can lead to a scattering between different transverse Laguerre-Gaussian modes $u_{\mu\nu}(r,\varphi)$, defined in Eq. (6), and thus the propagation of slow-light polaritons in a Rydberg gas in general has to be considered as a three-dimensional problem. In the following we will show that nevertheless an effective one-dimensional description is valid, provided the waist of the beam is small compared to the Rydberg blockade radius a_{B}.

To derive the interaction Hamiltonian of an effective one-dimensional model we use the decomposition of the spin coherence $\hat{\sigma}_{gr}(\mathbf{r})$ into Laguerre-Gaussian modes $\hat{\sigma}_{gr}(\mathbf{r}) = \sum_{\mu\nu} u_{\mu\nu}(r,\varphi)\hat{\sigma}_{gr}^{\mu\nu}(z)$ as in Sec. II B. This allows us to decompose the interaction into different components describing the

interaction between different transversal modes

$$\hat{H}_{\rm int} = \frac{n^2}{2}\int dz \int dz' \sum_{\substack{\mu_1\mu_2\mu_3\mu_4\\ \nu_1\nu_2\nu_3\nu_4}} \widetilde{V}^{\mu_1\mu_2\mu_3\mu_4}_{\nu_1\nu_2\nu_3\nu_4}(z-z') \times \hat{\sigma}^{\dagger\mu_1\nu_1}_{gr}(z)\hat{\sigma}^{\dagger\mu_2\nu_2}_{gr}(z')\hat{\sigma}^{\mu_3\nu_3}_{gr}(z')\hat{\sigma}^{\mu_4\nu_4}_{gr}(z), \quad (17)$$

The effective scattering matrix elements $\widetilde{V}^{\mu_1\mu_2\mu_3\mu_4}_{\nu_1\nu_2\nu_3\nu_4}$ are obtained from the three-dimensional interaction potential by integrating out r,r' and φ,φ',

$$\widetilde{V}^{\mu_1\mu_2\mu_3\mu_4}_{\nu_1\nu_2\nu_3\nu_4}(z-z') := C_6\int_0^{2\pi}d\varphi\int_0^{2\pi}d\varphi'\int_0^{\infty}rdr\int_0^{\infty}r'dr' \times \frac{u^*_{\mu_1\nu_1}(r,\varphi)u^*_{\mu_2\nu_2}(r',\varphi')u_{\mu_3\nu_3}(r',\varphi')u_{\mu_4\nu_4}(r,\varphi)}{[r^2+r'^2+2rr'\cos(\varphi-\varphi')+(z-z')^2]^3}. \quad (18)$$

The angular integrals can be calculated analytically by residue integration yielding the momentum conservation rule

$$\widetilde{V}^{\mu_1\mu_2\mu_3\mu_4}_{\nu_1\nu_2\nu_3\nu_4}(z-z') \propto \delta_{\mu_1-\mu_4,\mu_3-\mu_2}, \quad (19)$$

but further evaluation has to be done numerically. We are interested in the scattering processes of an initial Gaussian mode with zero angular momentum into higher-order Laguerre-Gaussian modes that are described by the scattering matrix elements $\widetilde{V}^{\mu,-\mu00}_{\nu_1\nu_200}$. The modes $u_{\mu\nu}$ with $\mu\neq 0$, i.e., higher-order azimuthal modes, have vanishing amplitude at $r=0$ and the corresponding interaction processes are suppressed compared to the $\mu=0$ modes. Thus we will restrict the following discussion to scattering processes into azimuthally symmetric modes.

In Fig. 2 we show the coupling strength of two photons at relative distance z in the Gaussian mode $\nu_3=\nu_4=0$ to Laguerre-Gaussian modes with radial indices ν_1,ν_2, calculated by numerical integration of (18). The relevant reference is the forward scattering potential $\widetilde{V}^{0,0,0,0}_{0,0,0,0}$. We find that for distances smaller than the beam waist w_0 all potentials show a z^{-4} decay with different initial amplitudes due to the small overlap of the different modes. At $z\approx w_0$ the potentials cross over to a power law $z^{-\alpha}$, where we find numerically that $\alpha\approx 6+2(\nu_1+\nu_2)$. Due to the strong interactions, excitations separated by small distances are blockaded, where typically the blockade distance is on the order of a few w_0. Therefore, the relevant distance regime is given by $w_0 < a_c \leqslant z$, where the scattering matrix elements scale as $z^{-\alpha}$. One recognizes that for distances already slightly larger than w_0 the scattering matrix elements into higher Laguerre-Gaussian modes are orders of magnitude smaller than the forward scattering one. Thus we can safely neglect the scattering processes into higher modes if the distance between excitations is sufficiently larger than the blockade radius $a_c > w_0$ [28]. The remaining potential $\widetilde{V}^{0000}_{0000}(r)$ can be approximated by the van der Waals potential $V(r)=C_6/|r|^6$ yielding an effective *one-dimensional* (1D) interaction. Omitting again the indices 0 we find

$$\hat{H}_{\rm int} = \frac{n^2}{2}\int dz\int dz' V(z-z')\hat{\sigma}^{\dagger}_{gr}(z)\hat{\sigma}^{\dagger}_{gr}(z')\hat{\sigma}_{gr}(z')\hat{\sigma}_{gr}(z). \quad (20)$$

Note that the 1D operators $\hat{\sigma}_{gr}(z)=\hat{\sigma}^{00}_{gr}(z)$ have a different physical dimension from the operators $\hat{\sigma}_{gr}(\mathbf{r})$ in three dimensions.

Transforming the 1D interaction Hamiltonian (20) to the polariton basis using $\sqrt{n}\hat{\sigma}_{gr}(z) = -\sin\theta\hat{\Psi}(z)+\cos\theta\hat{\Phi}(z)$ yields

$$\hat{H}_{\rm int} = \frac{1}{2}\int dz\int dz' V(z-z')\{[\sin\theta\hat{\Psi}^{\dagger}(z)-\cos\theta\hat{\Phi}^{\dagger}(z)] \times[\sin\theta\hat{\Psi}^{\dagger}(z')-\cos\theta\hat{\Phi}^{\dagger}(z')][\sin\theta\hat{\Psi}(z') - \cos\theta\hat{\Phi}(z')][\sin\theta\hat{\Psi}(z)-\cos\theta\hat{\Phi}(z)]\}. \quad (21)$$

By expanding the products one can identify terms describing (i) a two-body interaction of dark-state polaritons with relative strength $\sin^4\theta$, (ii) an interaction of bright-state polaritons with relative strength $\cos^4\theta$, and (iii) nonlinear coupling terms of dark- and bright-state polaritons.

In the slow-light regime one has $\cos^2\theta \ll 1$ and by taking the Hamiltonian (21) in lowest order of $\cos\theta$ only a nonlinear interaction term between Rydberg dark-state polaritons remains. Adding the effective free Hamiltonian that can be derived by adiabatically eliminating the bright-state polaritons from (10) and transforming to a frame comoving with the group velocity v_g finally yields

$$\hat{H}_{\rm eff} = -\int dz\ \hat{\Psi}^{\dagger}(z)\frac{\partial_z^2}{2m}\hat{\Psi}(z) + C_6\sin^4\theta\int dz\int dz'\frac{\hat{\Psi}^{\dagger}(z)\hat{\Psi}^{\dagger}(z')\hat{\Psi}(z')\hat{\Psi}(z)}{|z-z'|^6}, \quad (22)$$

where $m^{-1}\approx v_g L_{\rm abs}(\Delta/\gamma)$. This Hamiltonian was derived in [19] and used there as the basis of the theoretical discussion. It is, however, perturbative in the interaction-induced coupling between dark- and bright-state polaritons, which we will now analyze in more detail.

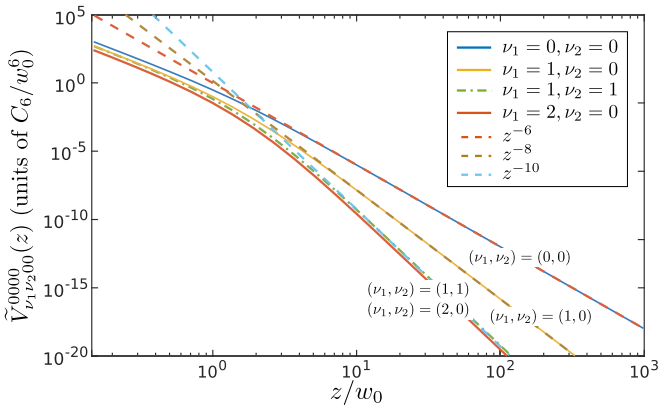

FIG. 2. (Color online) Different interaction potentials $\widetilde{V}^{0000}_{\nu_1\nu_2\nu_3\nu_4}$ between two photons initially in Laguerre-Gaussian modes ν_3,ν_4 sitting at positions $(z,z'=0)$ and finally in Laguerre-Gaussian modes ν_1,ν_2. In particular we choose initial Gaussian modes $\nu_3=\nu_4=0$ and final modes ν_1,ν_2 as labeled in the figure. The dashed lines indicate power-law fits $z^{-\alpha}$ in the regime $z>w_0$ with exponents $\alpha\in\{6,8,10\}$ (increasing slope). The potentials are symmetric in interchanging $\nu_1\leftrightarrow\nu_2$.

III. NONADIABATIC AND INTERACTION-INDUCED COUPLINGS

The derivation of Hamiltonian (22) requires the polaritons to keep a minimal distance of a_c defined in Eq. (16) to justify the approximations used in [19]. Two types of corrections arise due to the coupling between dark-state and bright-state polaritons: They are due to (i) nonadiabatic couplings that are already present in the noninteracting system and (ii) couplings between dark-state and bright-state polaritons induced by the interaction Hamiltonian (21).

Using the standard approach [29], we now derive an effective master equation for the Rydberg dark-state polaritons that allows us to treat both kinds of corrections at once. We will restrict ourselves to leading-order terms here. A brief derivation of the full master equation will be presented in the Appendix. The full time evolution of dark- and bright-state polaritons is governed by the sum of free Hamiltonian, which can be read off Eq. (10) and the interaction Hamiltonian (21) and can be decomposed into dark-state, bright-state, and coupling terms $\hat{H} = \hat{H}_0 + \hat{H}_{\rm int} = \hat{H}_\Psi + \hat{H}_\Phi + \hat{H}_{\Psi\Phi}$. The free time evolution of the polaritons in zeroth order in the coupling is described by the differential equations (10),

$$\partial_t \hat{\Psi}(z,t) = -c\cos^2\theta\,\partial_z \hat{\Psi}(z,t),$$
$$\partial_t \hat{\Phi}(z,t) = -c\sin^2\theta\,\partial_z \hat{\Phi}(z,t) - \Gamma_{\rm eff}\hat{\Phi}(z,t),$$

where we have disregarded the Langevin noise terms. As can easily be shown, the solution of these equations is given by $\hat{\Psi}(z,t) = \hat{\Psi}(z - c\cos^2\theta\tau, t-\tau)$ and $\hat{\Phi}(z,t) = e^{-\Gamma_{\rm eff}\tau}\hat{\Phi}(z - c\sin^2\theta\tau, t-\tau)$. Thus the free dark-state polaritons propagate form-stable with group velocity $v_g = c\cos^2\theta$, while the bright-state polaritons propagate with velocity $c\sin^2\theta$ and are subject to radiative decay with rate $\mathrm{Re}[\Gamma_{\rm eff}]$. Assuming that $|\Gamma_{\rm eff}|^{-1}$ defines the fastest time scale, we can adiabatically eliminate the bright-state polaritons. If there is no external driving of bright-state polaritons, they decay into the vacuum state $\rho_\Phi = |\mathrm{vac}\rangle_\Phi\langle\mathrm{vac}_\Phi|$ for which the lowest-order correlation function reads

$$\langle\hat{\Phi}(x,t)\hat{\Phi}^\dagger(y,t-\tau)\rangle \approx e^{-\Gamma_{\rm eff}\tau}\delta(x-y), \quad \tau > 0. \tag{23}$$

The remaining nonvanishing correlation functions can be found in the Appendix, Eq. (A1).

In an interaction picture with respect to $\hat{H}_\Psi + \hat{H}_\Phi$ the dark-state polariton degrees of freedom are described by the density matrix $\rho = \mathrm{tr}_\Phi(\chi)$. In the Born approximation the time evolution of ρ is then governed by

$$\dot{\rho}_\Psi(t) = -\int_0^\infty d\tau\,\mathrm{tr}_\Phi\{[\hat{H}_{\Psi\Phi}(t),[\hat{H}_{\Psi\Phi}(t),\rho(t)\otimes\rho_\Phi]]\}. \tag{24}$$

We note that the free part of $\hat{H}_\Psi$ corresponds to the generator of a transformation to a frame comoving with the group velocity $v_g = c\cos^2\theta$. Introducing the operator

$$\hat{L} \equiv -\sin^3\theta\cos\theta\left[\int ds\, V(z-s)\hat{\Psi}^\dagger(s)\hat{\Psi}(s) + i\frac{c\partial_z}{\sin^2\theta}\right]\hat{\Psi}(z) \tag{25}$$

allows us to write the system-reservoir-coupling Hamiltonian in the interaction picture in the compact form

$$\hat{H}_{\Psi\Phi}(t) = \int dz\{\hat{\Phi}^\dagger(z)\hat{L}(z) + \hat{L}^\dagger\hat{\Phi}(z)\} + \cdots, \tag{26}$$

where we neglected terms of second and higher order in the bright-state polariton operators. We insert Eq. (26) into Eq. (24) and follow the standard derivation of a master equation [29]. Performing the Markov approximation, we get a master equation in Lindblad form describing an effective time evolution of the dark-state polaritons. After transforming back to a moving frame we arrive at

$$\dot{\rho} = i\frac{\Delta}{\Omega_e^2}\int dz[\rho,\hat{L}^\dagger(z)\hat{L}(z)] + i\sin^4\theta\int dz\int dz' \times V(z-z')[\rho,\hat{\Psi}^\dagger(z)\hat{\Psi}^\dagger(z')\hat{\Psi}(z')\hat{\Psi}(z)] + \frac{\gamma}{\Omega_e^2}\int dz(2\hat{L}(z)\rho\hat{L}^\dagger(z) - \{\rho,\hat{L}^\dagger(z)\hat{L}(z)\}), \tag{27}$$

where $\{\cdot,\cdot\}$ denotes the anticommutator and we have taken into account only leading-order terms in $\cos^2\theta \ll 1$. Specifically, the unitary time evolution is governed by $\hat{L}^\dagger(z)\hat{L}(z)\Delta/\Omega_e^2$ and the dark-state polariton interaction in the second line of Eq. (27). After expanding $\hat{L}^\dagger(z)\hat{L}(z)$ we identify the following terms: first, a kinetic energy term with an effective mass

$$m^{-1} = 2v_g\frac{c\Delta\sin^2\theta}{\Omega_e^2} = 2v_g\frac{\Delta}{\gamma}L_{\rm abs}\sin^4\theta; \tag{28}$$

second, a drift term proportional to $\int dz' V(z-z')\hat{\Psi}^\dagger(z')\hat{\Psi}(z')$, giving corrections to the group velocity v_g mediated by interactions in the presence of a second polariton; and, finally, higher-order terms in the interaction, namely, a three-body interaction and corrections to the two-body interaction proportional to $V^2(z-z')$. Combining the two-body interaction terms, we find the effective potential

$$V_{\rm eff}(r) \approx \sin^4\theta\left[V(r) + \frac{\Delta}{\Omega_e^2}\cos^2\theta\,V^2(r)\right]. \tag{29}$$

As can be seen from this, the second correction term becomes relevant for distances smaller than $r_0 = (|C_6\Delta|\cos^2\theta/\Omega_e^2)^{(1/6)}$, where the potential leads to an r^{-12} interaction. Note that this interaction is always repulsive for $r < r_0$, since the product of the effective mass and effective potential is always positive for $r < r_0$. Thus, independent of the signs of the detuning and the C_6 coefficient, Rydberg dark-state polaritons are always expelled from the region of small relative distances.

The bright-state polaritons are subject to radiative decay giving rise to effective loss channels for the dark-state polaritons. The decay processes are described by the operator $\hat{L}$ defined in (25). This operator consists of two terms corresponding to the two possible loss channels resulting from coupling between dark- and bright-state polaritons, namely, a linear coupling that becomes relevant outside the EIT window and a nonlinear coupling arising from the interaction. In particular, we identify a generalized single-particle decay generated by the Lindblad operator $\sqrt{\hat{\Gamma}(z)}\hat{\Psi}(z)$ with the

operator-valued loss rate

$$\hat{\Gamma}(z) = \frac{\gamma \cos^2\theta \sin^6\theta}{\Omega_e^2}\left[\int dx\, V(z-x)\hat{\Psi}^\dagger(x)\hat{\Psi}(x)\right]^2. \quad (30)$$

Note that these losses as well as the corrections to the drift term cannot be simply treated in a mean-field approximation, since $V(r)$ diverges for $r \to 0$. For a physical interpretation of the losses we assume a fixed Rydberg excitation $\hat{\Psi}^\dagger(x)\hat{\Psi}(x) = \sin^2\theta\delta(x)$, which yields a loss rate $\Gamma(r) \approx \gamma\cos^2\theta V^2(r)/\Omega_e^2$ for a dark-state polariton at a distance r from the fixed excitation, which scales like r^{-12}. The remaining loss terms include the spatial derivative $\partial_z\hat{\Psi}$ as well a combination thereof and the interaction potential. Thus they can be interpreted as momentum-dependent damping terms affecting high-energy modes strongly.

We have shown that treating the bright-state polaritons as a reservoir for the dark-state polaritons allows us to derive the effective Hamiltonian (22) with corrections. The leading-order corrections are a strong repulsive potential as well as a strong loss process for short relative distances scaling as r^{-12}, which leads to a strong blockade effect. The nature of the blockade effect is determined by the ratio of Δ/γ. In the far-off-resonance regime ($\Delta \gg \gamma$) strong repulsion dominates, while in the resonant regime ($\Delta \ll \gamma$) absorption dominates.

We point out that the master equation approach distinguishes explicitly between dissipative and unitary time evolution, other than a simple perturbative calculation that yields a complex polariton mass.

IV. TWO-PARTICLE SIMULATIONS AND VERIFICATION OF THE EFFECTIVE MODEL

It was shown numerically in [30] and on the basis of an effective master equation that the van der Waals interaction leads to an avoided volume for the propagating photons. Near single-photon resonance $|\Delta| \leqslant \gamma$, two photons at distance smaller than a_B get absorbed and an incident two-photon wave packet evolves into a nonclassical state that is a statistical mixture of a single excitation and a correlated train of (two) photons separated by $2a_B$ [30]. In the off-resonance regime ($|\Delta| \gg \gamma$) the absorption plays no role but two photons closer than the blockade distance propagate with the vacuum speed of light and thus escape from the remaining wave packet, which lags behind. Moreover, the repulsive interaction prevents the photons from getting inside the blockade distance.

To validate this picture we perform numerical simulations of the full 1D Maxwell-Bloch equations for two copropagating polaritons subject to van der Waals interaction. We consider an initial Gaussian two-photon wave packet $[|\Psi_0\rangle = EE(z_1,z_2,t)\hat{\mathcal{E}}^\dagger\hat{\mathcal{E}}^\dagger|0\rangle]$ in free space, i.e., $EE(z_1,z_2,t) \propto e^{-(z_1-ct)^2/2l_p}e^{-(z_2-ct)^2/2l_p}$, where we assume that the spectral width fits well inside the EIT window of the medium in the absence of interactions. The state vector at time t is then described by the two-excitation wave function

$$|\Psi(t)\rangle = \int dz_1 \int dz_2 \sum_{F,G} FG(z_1,z_2,t)\hat{F}^\dagger(z_1)\hat{G}^\dagger(z_2)|0\rangle,$$

where $\hat{F},\hat{G} \in \{\hat{\mathcal{E}},\hat{\sigma}_{ge},\hat{\sigma}_{gr}\}$ and $FG(z_1,z_2,t) = \langle\Psi(t)|\hat{F}^\dagger(z_1)\hat{G}^\dagger(z_2)|0\rangle$ denotes all possible two-particle wave functions corresponding to excitations in the electric field $\hat{\mathcal{E}}$ (E), the polarization $\hat{\sigma}_{ge}$ (P), and the spin coherence $\hat{\sigma}_{gr}$ (S), respectively. For example, $|EE(z_1,z_2,t)|^2$ gives the probability of finding two electric-field excitations at positions z_1 and z_2, i.e., $FG \in \{EE,PP,SS,EP,PE,ES,SE,PS,SP\}$. Note that in the presence of decay the norm of the wave function is not conserved. We then simulate the propagation of the pulse from free space into the Rydberg gas by considering a space-dependent atomic coupling strength $g^2n = g^2n(z)$, where we use a step function in space for $n(z)$. To take care of the EIT pulse compression for small group velocities we employ an adaptive spatial grid spacing. In Figs. 3(a) and 3(b) we show two snapshots of the time evolution of the $EE(z_1,z_2)$ component incident into the medium in the lower left corner

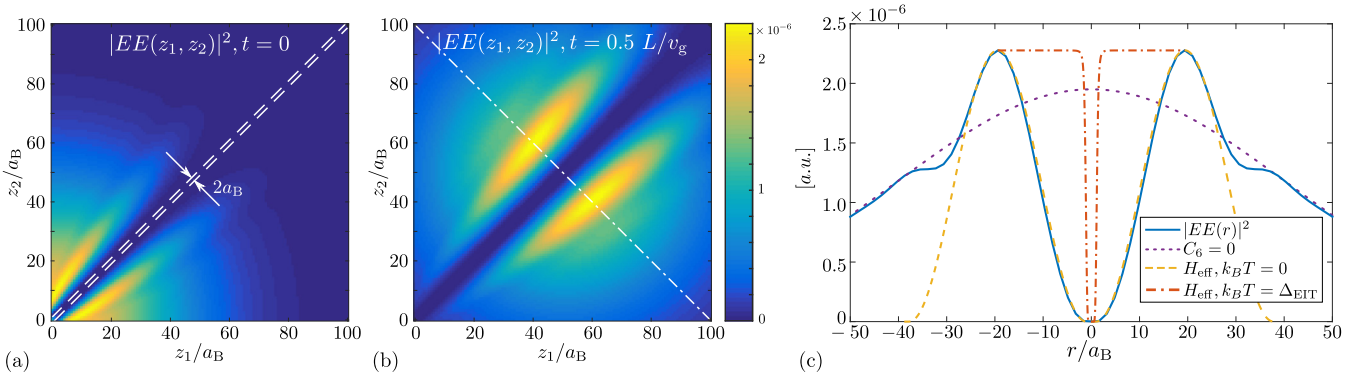

FIG. 3. (Color online) Splitting of the initial Gaussian wave packet due to van der Waals interaction. The full two-excitation wave function simulation is shown for the parameters $g = 10\Omega = 10\gamma$ and $\Delta = 4\gamma$. The optical depth per blockade is chosen as $d_B \equiv a_B/L_{abs} = 7$. The color plots show the two-excitation probe field amplitude $EE(z_1,z_2,t)$ at times (a) $t = 0$ and (b) $t = 0.5L/v_g$ corresponding to the times where the center of the incident Gaussian wave packet is at the medium boundary and at the middle of the medium, respectively. (c) Cross section (blue solid line) of the middle color plot along the diagonal $r = z_1 - z_2$ for $2R = z_1 + z_2 = L = 100a_B$, as indicated by the dash-dotted line in (b). We compare the cross section to a pulse propagating in the absence of interactions (Gaussian, purple dotted line) and the two-particle ground state of the effective Hamiltonian (22) (yellow dashed line), where we impose periodic boundary conditions with a period corresponding to the distance of the two peaks (blue solid line). The red dash-dotted line shows a thermal two-particle state of the effective Hamiltonian. For illustration purposes we continued the two-particle ground state.

($z_{1/2} = 0$) and propagating along the diagonal to the upper right corner of the pictures. As can be seen, in the considered off-resonance regime, the wave packet splits at the medium boundary into two parts separated by $2a_B$, indicating a photon antibunching as shown for the resonant case in [30]. However, after longer propagation inside the medium the separated parts move even farther apart due to the repulsive interaction on length scales $\Delta z \gg a_B$.

The results in Fig. 3 verify the expected time evolution governed by the Hamiltonian (22). This can be seen from Fig. 3(c), where we compare a cross section (blue solid line) of the evolved pulse to the two-excitation ground state of the effective Hamiltonian (yellow dashed line) calculated for periodic boundary conditions. For illustrative purposes we have periodically continued the ground-state wave function in the plot.

We recognize two important things. First, we find remarkably good agreement between the numerically evolved wave packet and the ground state of the effective Hamiltonian up to a length scale of $r \approx \pm 25 a_B$. Second, we do not find localized two-particle excitations around $r = 0$ (bunching), contrary to [12].

That the final state of the evolution is so close to the ground state is somewhat unexpected since the initial wave packet contains many highly excited components. The presence of a finite EIT window sets an upper bound on the energy of the polaritons. Since the system is not integrable, we can assume that the polaritons quickly thermalize after entering the interacting medium. However, as can be seen from a comparison with the red dash-dotted curves in Fig. 3(c), a temperature estimated by the EIT transmission window (11) is much too high. A possible explanation for this is the presence of a mechanism similar to evaporative cooling. High-energy modes of the dark-state polaritons are preferentially coupled to bright-polariton modes and decay or propagate away. Further analysis of this mechanism is beyond the scope of the present paper.

Let us briefly comment on the fact that we do not see bunching of photons in the numerical simulations of the full Maxwell-Bloch equations as demonstrated in [12]. Here we consider the case $mC_6 > 0$, where the effective Hamiltonian (22) does not have bound states that would support bunching. The full set of Maxwell-Bloch equations, on the other hand, should reproduce the bunching. However, our simulation is run in a regime where the optical depth per blockade $d_B = a_B/L_{abs}$ is much larger than in [12]. As will be discussed elsewhere [27], in this regime not a single but many bound states exist, which cannot be excited, however, by the incident photon pulse. For values of d_B much smaller than considered here we also find bunching in our numerics [27].

V. LIGHT STORAGE IN RYDBERG GASES

A. Reaching the strongly interacting regime

The physics of the polariton Hamiltonian (22) is governed by an interplay of the kinetic energy contribution trying to delocalize the massive particles and the polariton-polariton interaction leading to spatial order. If the kinetic energy per particle dominates, the polaritons are in the weakly interacting regime, characterized by small quantum correlations. An interesting question is if one can also reach the opposite limit of strong correlations, where interactions set the dominant energy scale. To answer this question we make use of the fact that the low-energy physics of a gapless one-dimensional system can be described in terms of a Luttinger liquid (LL) [31].

A LL is fully characterized by two parameters, the speed of sound v_s and the Luttinger parameter K; K universally determines the long-range behavior of the ground state correlation functions. In particular, the equal-time first-order correlation function describing superfluid order is given by [31]

$$\langle \hat{\Psi}^\dagger(z)\hat{\Psi}(0)\rangle = \rho_0 A_1 \left(\frac{1}{z}\right)^{1/2K}, \tag{31}$$

where the amplitude A_1 is some nonuniversal constant. Likewise, one finds for the density-density correlations

$$\langle \hat{\rho}(z)\hat{\rho}(0)\rangle = \rho_0^2 - \frac{K}{2\pi^2}\frac{1}{z^2} + A_2\rho_0^2 \cos(2\pi\rho_0 z) z^{-2K}, \tag{32}$$

where $\hat{\rho}(z) = \hat{\Psi}^\dagger(z)\hat{\Psi}(z)$ and A_2 is again a nonuniversal amplitude. We are particularly interested in the last term in Eq. (32), which oscillates spatially with the period $1/\rho_0$ corresponding to a charge-density wave (CDW). Depending on K either superfluid (first-order) ($K \gg 1/2$) correlations or CDW order ($K \ll 1/2$) dominate long-range correlations and $K = 1/2$ marks the crossover point where both correlations decay with an exponent 1. Further, $K \gg 1$ corresponds to a gas of weakly interacting bosons, where superfluid order dominates, and $K = 1$ to a gas of either hard-core bosons, i.e., bosons with infinite local interactions, or equivalently to free fermions, which are dual to each other. Note that values of K less than unity cannot be reached for pointlike interactions, such as photons interacting via a Kerr nonlinearity [32,33].

In Fig. 4 we show normalized density-density and first-order correlations calculated by density-matrix renormalization-group (DMRG) simulations. For short distances the normalized density-density correlations are strongly suppressed, i.e., $g^{(2)}(0) = 0$, indicating the photon blockade of two copropagating excitations. Here we have introduced a dimensionless parameter Θ, defined as the ratio of the interaction energy at average interparticle distance $1/\rho_0$ and the Fermi energy [34],

$$\Theta = \frac{(\rho_0 a_B)^4}{4\pi}\left(\frac{\gamma}{\Delta}\right)^2 d_B^2. \tag{33}$$

For small Θ, corresponding to weak interactions, the first-order correlation functions govern the long-range behavior, indicating a superfluid state. Increasing the interaction strength leads to a strongly pronounced and slowly decaying density wave (CDW) with fast decaying first-order correlations. Due to the low (one) dimensionality of the model, no slower-than-power-law decay of correlations can be found, i.e., the model cannot exhibit true crystalline order. The latter can in principle be created by engineering an additional lattice potential, i.e., a space-dependent two-photon detuning for the polaritons leading to a sine-Gordon-like model for commensurate fillings. This model exhibits a quantum phase transition to a gapped phase with true crystalline order [31,35].

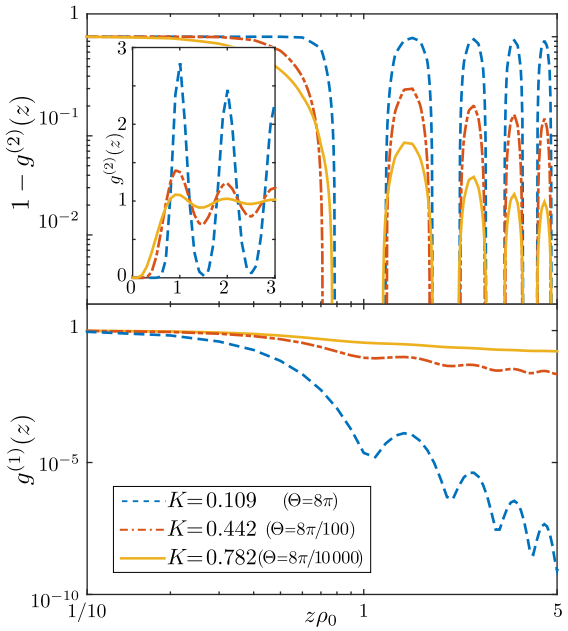

FIG. 4. (Color online) Correlation functions computed by DMRG. The top panel shows $1-g^{(2)}(z)$ [and $g^{(2)}(z)$ in the inset] for different interaction strengths as labeled in the legend in the bottom plot, where $g^{(2)}$ is the normalized density-density correlation (taken from [19]). The bottom panel shows the corresponding first-order correlation functions for different interaction strengths as labeled in the legend.

To enter the strongly interacting regime $K \ll 1$ has to be realized, which is only possible for nonlocal interactions such as the $1/r^6$ interactions of Rydberg polaritons. As we will discuss in the following section, this regime, however, is not accessible for Rydberg polaritons under typical cw EIT conditions.

B. Strongly interacting regime under stationary EIT conditions

We now discuss what LL parameters can be reached in a gas of Rydberg polaritons. For our model (22), the dependence of the K parameter as a function of microscopic parameters cannot be given analytically, but has to be determined numerically. We can extract K from DMRG simulations, where we calculate the compressibility $\chi^{-1} = \rho_0^2 \frac{\partial \mu}{\partial \rho_0} = \rho_0^2 L \frac{\partial^2 E}{\partial N^2}$. From this we get the ratio $K/v_s = \pi\rho_0^2\chi$ and together with the product $v_s K = \pi\rho_0/m$, which is constant for any Galilean invariant system [31], we can extract the K parameter as a function of Θ. For power-law interactions an approximate analytical formula for the K parameter has been given in [36], which is asymptotically correct for small and large Θ,

$$K = \left(1 + \frac{\pi^4}{45}\Theta\right)^{-1/2}. \tag{34}$$

From this we can estimate the experimental requirements for reaching the strongly interacting regime ($K \ll 1$) under stationary EIT conditions. An important restriction of stationary EIT is set by the Rydberg blockade: When two excitations get closer than the EIT blockade radius a_B [Eq. (15)] they are either absorbed or transformed into fast propagating bright-state

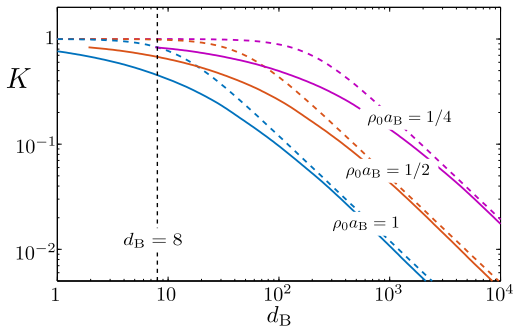

FIG. 5. (Color online) Plot of the K parameter as a function of the optical depth per blockade d_B for $\Delta/\gamma = 10$. Solid curves are interpolated numerical data from DMRG results and the corresponding dashed curves are approximate values according to (34). The three pairs of curves are for different values $\rho_0 a_B$ as labeled in the plot. The dashed vertical line indicates experimental values from [11].

polaritons that escape. Thus the excitation density is limited to values

$$\rho_0 a_B \leqslant 1 \tag{35}$$

and in the regime of small K we have $K \sim d_B^{-1}$, indicating that even for a large density ($\rho_0 a_B \approx 1$) the required optical depth per blockade is orders of magnitude higher than experimentally feasible [11] (cf. Fig. 5). Moreover, increasing d_B by changing the blockade distance a_B requires a smaller excitation density ρ_0 for fixed $\rho_0 a_B$ and thus limits the number of excitations in a finite-length medium such that in the limit $d_B \gg 1$ only a single excitation would be allowed inside the medium for stationary EIT driving.

C. Frequency pulling in the adiabatic slowdown of Rydberg polaritons

The problem of reaching the required conditions for quasicrystalline order of Rydberg polaritons under stationary EIT conditions can be overcome using a *dynamical* protocol, i.e., by light storage or dynamical slowdown of polaritons inside the medium. One recognizes from (15) that during slowdown and ultimately light storage the EIT blockade radius $a_B \propto \Omega^{-1/3}$ diverges. Naively one would expect that as a consequence the smallest possible distance between Rydberg polaritons diverges as well. Remarkably this is not the case. To see this, let us consider the dynamics of a dark-state polariton pulse during storage with an initial fixed nonzero two-photon detuning $\omega_p(0) + \omega_c - \omega_{rg} = \delta_0$, resulting, e.g., as an interaction shift from a second Rydberg polariton. As has been shown in [37], a small two-photon detuning causes a time-dependent phase shift (chirp) of the dark-state polariton during slowdown:

$$\hat{\Psi}(z,t) = \hat{\Psi}\left(z - c\int_0^t d\tau \cos^2[\theta(\tau)], 0\right) \times \exp\left\{i\delta_0 \int_0^t d\tau \sin^2[\theta(\tau)]\right\}. \tag{36}$$

As a consequence of this the spectrum of the probe field $\hat{\mathcal{E}}(z,t) = \cos\theta(t)\hat{\Psi}(z,t)$, assuming a slowly varying mixing

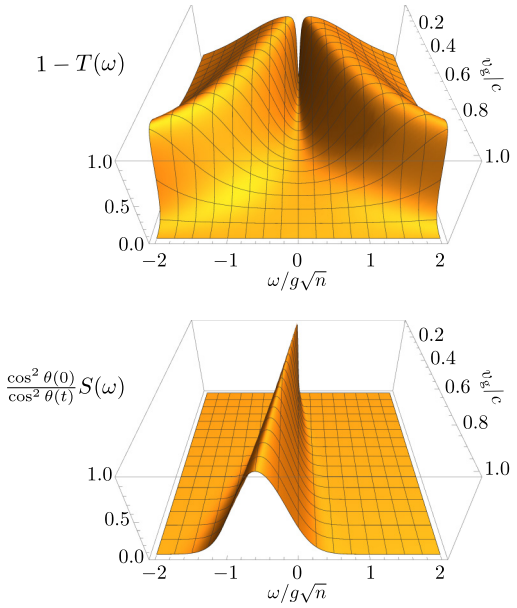

FIG. 6. (Color online) Illustration of the transmission spectrum $T(\omega)$ of the EIT medium (top) and normalized spectrum $S(\omega)/\cos^2\theta$ of the electromagnetic field (bottom) in arbitrary units as a function of the normalized group velocity $v_g/c = \cos^2\theta$ during a dynamical light storage protocol. Here δ denotes the detuning from the two-photon resonance $\omega_p + \omega_c = \omega_{rg}$.

angle $\theta(t)$, can be expressed as

$$S(z,\omega) = \int_{-\infty}^{\infty} d\tau\, e^{-i\omega\tau}\langle\hat{\mathcal{E}}^\dagger(z,t)\hat{\mathcal{E}}(z,t-\tau)\rangle = \frac{\cos^2\theta(t)}{\cos^2\theta(0)} S\left(0, \frac{1}{\cos^2\theta(t)}[\omega + \delta_0\sin^2\theta(t)]\right). \quad (37)$$

One recognizes two effects. First, there is a spectral narrowing proportional to $\cos^2\theta(t)$, which guarantees that during light storage the pulse spectral width remains less than the EIT transparency window (11), if it did so at the beginning of the storage process [38]. Second, there is a pulling of the center frequency of the pulse towards the two-photon resonance

$$\omega_p(t) = \omega_p(0) - \delta_0\sin^2\theta(t), \quad (38)$$

$$\delta(t) = \omega_p(t) + \omega_c - \omega_{rg} = \delta_0\cos^2\theta(t) \to 0. \quad (39)$$

Frequency pulling and spectral narrowing are illustrated in Fig. 6, where we have plotted schematically the transmission spectrum $T(\delta)$ and the spectrum of the probe pulse $S(\delta)$, where $\delta = \delta(t)$ denotes the detuning from two-photon resonance, as a function of the normalized group velocity. This effect has been observed experimentally in [39] and is responsible for the fact that the two-photon linewidth of EIT light storage [37] is determined by the collective Rabi frequency Ω_e rather than the control-field Rabi frequency $\Omega(t)$: $\delta_{ph} = \Omega_e^2/|\Gamma|$. (Here we have set the optical depth $d = 1$.)

As a consequence of this the minimum distance of two Rydberg polaritons is not given by the EIT blockade distance (15) but by the critical distance

$$a_c = \sqrt[6]{|C_6\Gamma|/\Omega_e^2}. \quad (40)$$

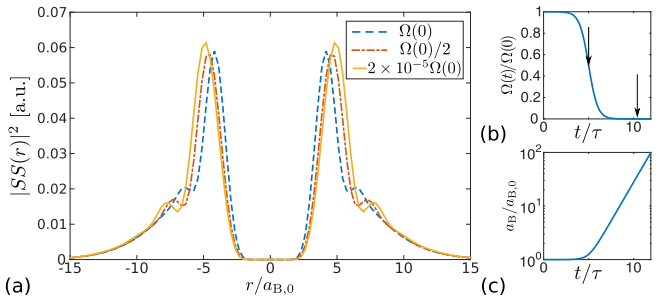

FIG. 7. (Color online) Plot of the SS component of the two-particle wave function during storage. (a) Spatial distribution of the doubly excited spin component for three different times: after an initial transient but before starting the storage protocol (blue dashed line); at time t_0, where $\Omega(t_0) = \frac{1}{2}\Omega_0$ (red dash-dotted line); and at the end of the protocol (yellow solid line), where $\Omega(t)$ is approximately zero as indicated by the arrows in (b). (b) Time dependence of the control field, which is turned off according to $\Omega(t) = \frac{\Omega_0}{2}\{1 - \tanh[(t-t_0)/\tau]\}$. The blockaded distance during storage stays finite while the stationary blockade radius $a_B \propto \Omega^{-1/3}$ diverges as shown in (c).

We have verified this by two-particle simulations, which are illustrated in Fig. 7. Shown is the spin-spin component of an initial two-photon wave packet propagating in an EIT medium with Rydberg interactions as in Sec. IV. After an initial transient an avoided volume is formed corresponding to the blockade radius $a_B(\Omega_0)$ given by the *initial* drive-field Rabi frequency Ω_0 and larger than the critical distance a_c (cf. Fig. 3). When the drive field is adiabatically turned to zero as shown in Fig. 7(b), the EIT blockade radius $a_B(\Omega(t))$ increases and eventually diverges [see Fig. 7(c)]. The avoided volume, however, stays approximately constant. This shows that an adiabatic slowdown of Rydberg polaritons allows us to increase their effective mass and thus the ratio of the interaction energy to kinetic energy Θ, without reducing the polariton density ρ_0. In this way it is possible to enter the interesting regime of strong interactions between Rydberg dark-state polaritons [19].

VI. SUMMARY

We derived an effective model for the interaction of photons in a gas of Rydberg atoms under conditions of electromagnetically induced transparency in particular in the regime of large optical depth per blockade distance $d_B \gg 1$. We showed that under paraxial propagation conditions and for sufficiently low densities of excitations the system can be described by an effective model of a single species of quasiparticles, called Rydberg dark-state polaritons. The model can be reduced to one spatial dimension if the transverse beam diameter is less than the EIT blockade radius. For sufficiently large interparticle distances Rydberg polaritons behave as massive Schrödinger particles with repulsive van der Waals–type interactions. For shorter distances there is a coupling of dark-state polaritons to decaying and fast propagating bright-state polaritons, giving rise to an effective loss mechanism for Rydberg polaritons. For an off-resonance excitation scheme with finite single-photon detuning, also bound two-particle states exist. As will be

discussed in detail elsewhere [27] these states cannot be excited for large d_B from an initial light field and thus were not considered here. We derived conditions where the losses in the effective Rydberg polariton model are negligible and we can use an effective Hamiltonian. The ground-state properties of this Hamiltonian were analyzed using numerical DMRG simulations and in terms of a Luttinger-liquid model. We showed that the regime of strong interactions, characterized by a large ratio of interaction to kinetic energy $\Theta \gg 1$, is very difficult to reach under stationary EIT conditions. Increasing the strength of the van der Waals interaction between Rydberg atoms leads to an increase of the EIT blockade distance, which prevents reaching sufficiently large polariton densities inside the medium under stationary EIT conditions.

However, making use of a dynamical slowdown of Rydberg polaritons propagating inside the medium or a storage protocol of polaritons into stationary spin excitations allows us to decrease the kinetic energy by increasing their effective mass without reducing the quasiparticle density. In this way it is possible to generate a quasicrystalline or charge-density wave state of stored photons, which is a highly nonclassical state consisting of an ordered string of single-photon wave packets. This state can be observed either by nonadiabatic release of the stored excitations into a train of single photons or by direct imaging of the Rydberg ensemble as in [40].

ACKNOWLEDGMENTS

We thank J. Otterbach, S. Whitlock, M. Weidemüller, and H. P. Büchler for valuable discussions. The financial support of the Deutsche Forschungsgemeinschaft through Grant No. SFB/TR49 is gratefully acknowledged.

APPENDIX: DERIVATION OF THE FULL MASTER EQUATION

Here we present a brief derivation of the full version of the master equation (27) including higher-order terms that have been neglected in Sec. III.

In addition to the first-order correlation function (23) of two operators the only nonvanishing correlation function arising in evaluating Eq. (24) is the antinormal-ordered correlation function of four bright-state polariton operators

$$\langle\hat{\Phi}(x,t)\hat{\Phi}^\dagger(y,t-\tau)\rangle \approx e^{-\Gamma_{\rm eff}\tau}\delta(x-y), \quad \tau>0, \tag{A1}$$

$$\begin{aligned}\langle\hat{\Phi}(x,t)\hat{\Phi}(x',t)\hat{\Phi}^\dagger(y,t-\tau)\hat{\Phi}^\dagger(y',t-\tau)\rangle \\ \approx e^{-2\Gamma_{\rm eff}\tau}[\delta(x-y-v\tau)\delta(x'-y'-v\tau) \\ +\delta(x'-y-v\tau)\delta(x-y'-v\tau)], \quad \tau>0.\end{aligned} \tag{A2}$$

The interaction Hamiltonian $\hat{H}_{\Psi\Phi}$ including terms quadratic in bright-state polaritons is given by

$$\begin{aligned}\hat{H}_{\Psi\Phi}(t) = \int dz\Big(\hat{\Phi}^\dagger(z)\hat{L}(z)+\hat{L}^\dagger\hat{\Phi}(z)+\int dz' V(z-z') \\ \times \sin^2\theta\cos^2\theta(\hat{\Phi}^\dagger(z,t)\hat{\Phi}^\dagger(z',t)\hat{\Psi}(z',t)\hat{\Psi}(z,t) \\ +\hat{\Psi}^\dagger(z,t)\hat{\Psi}^\dagger(z',t)\hat{\Phi}(z',t)\hat{\Phi}(z,t))\Big).\end{aligned} \tag{A3}$$

The full Hamiltonian includes additional terms cubic in bright-state polaritons. These terms are not relevant to the time evolution of dark-state polaritons since three-particle correlations of bright-state polaritons vanish in the vacuum. Using the Hamiltonian (A3) in Eq. (24), we find the full master equation

$$\begin{aligned}\dot{\rho} = i\frac{\Delta}{\Omega_e^2}\int dz[\rho,\hat{L}^\dagger(z)\hat{L}(z)] + i\sin^4\theta\int dz\int dz' \\ \times V(z-z')[\rho,\hat{\Psi}^\dagger(z)\hat{\Psi}^\dagger(z')\hat{\Psi}(z')\hat{\Psi}(z)] \\ +i\frac{\Delta\sin^4\theta\cos^4\theta}{\Omega_e^2}\int dz\int dz' V^2(z-z') \\ \times[\rho,\hat{\Psi}^\dagger(z)\hat{\Psi}^\dagger(z')\hat{\Psi}(z')\hat{\Psi}(z)] \\ +\frac{\gamma}{\Omega_e^2}\int dz[2\hat{L}(z)\rho\hat{L}^\dagger(z)-\{\rho,\hat{L}^\dagger(z)\hat{L}(z)\}] \\ +\frac{\gamma\sin^4\theta\cos^4\theta}{\Omega_e^2}\int dz\int dz' V^2(z-z')[2\hat{\Psi}(z')\hat{\Psi}(z) \\ \times\rho\hat{\Psi}^\dagger(z)\hat{\Psi}^\dagger(z')-\{\rho,\hat{\Psi}^\dagger(z)\hat{\Psi}^\dagger(z')\hat{\Psi}(z')\hat{\Psi}(z)\}],\end{aligned} \tag{A4}$$

including higher-order corrections. The additional terms compared to Eq. (27) are a correction to the two-particle interaction potential in the second line as well as a two-particle loss in the last line of Eq. (A4). Both terms are proportional to $\cos^4\theta$ and thus are highly suppressed in the case of slow light.

[1] T. F. Gallagher, *Rydberg Atoms* (Cambridge University Press, Cambridge, 1994).
[2] M. G. Bason, A. K. Mohapatra, K. J. Weatherill, and C. S. Adams, Phys. Rev. A **77**, 032305 (2008).
[3] J. D. Pritchard, D. Maxwell, A. Gauguet, K. J. Weatherill, M. P. A. Jones, and C. S. Adams, Phys. Rev. Lett. **105**, 193603 (2010).
[4] S. Sevinçli, N. Henkel, C. Ates, and T. Pohl, Phys. Rev. Lett. **107**, 153001 (2011).
[5] D. Petrosyan, J. Otterbach, and M. Fleischhauer, Phys. Rev. Lett. **107**, 213601 (2011).
[6] B. Olmos, W. Li, S. Hofferberth, and I. Lesanovsky, Phys. Rev. A **84**, 041607(R) (2011).
[7] J. Honer, R. Löw, H. Weimer, T. Pfau, and H. P. Büchler, Phys. Rev. Lett. **107**, 093601 (2011).
[8] C. S. Hofmann, G. Günter, H. Schempp, M. Robert-de-Saint-Vincent, M. Gärttner, J. Evers, S. Whitlock, and M. Weidemüller, Phys. Rev. Lett. **110**, 203601 (2013).
[9] D. Maxwell, D. J. Szwer, D. Paredes-Barato, H. Busche, J. D. Pritchard, A. Gauguet, M. P. A. Jones, and C. S. Adams, Phys. Rev. A **89**, 043827 (2014).
[10] M. F. Maghrebi, N. Y. Yao, M. Hafezi, T. Pohl, O. Firstenberg, and A. V. Gorshkov, Phys. Rev. A **91**, 033838 (2015).
[11] T. Peyronel, O. Firstenberg, Q.-Y. Liang, S. Hofferberth, A. V. Gorshkov, T. Pohl, M. D. Lukin, and V. Vuletic, Nature (London) **488**, 57 (2012).

[12] O. Firstenberg, T. Peyronel, Q.-Y. Liang, A. V. Gorshkov, M. D. Lukin, and V. Vuletic, Nature (London) **502**, 71 (2013).
[13] S. Baur, D. Tiarks, G. Rempe, and S. Dürr, Phys. Rev. Lett. **112**, 073901 (2014).
[14] D. Tiarks, S. Baur, K. Schneider, S. Dürr, and G. Rempe, Phys. Rev. Lett. **113**, 053602 (2014).
[15] H. Gorniaczyk, C. Tresp, J. Schmidt, H. Fedder, and S. Hofferberth, Phys. Rev. Lett. **113**, 053601 (2014).
[16] D. Paredes-Barato and C. S. Adams, Phys. Rev. Lett. **112**, 040501 (2014).
[17] E. Shahmoon, G. Kurizki, M. Fleischhauer, and D. Petrosyan, Phys. Rev. A **83**, 033806 (2011).
[18] G. Epple, K. S. Kleinbach, T. G. Euser, N. Y. Joly, T. Pfau, P. St. J. Russel, and R. Löw, Nat. Commun. **5**, 4132 (2014).
[19] J. Otterbach, M. Moos, D. Muth, and M. Fleischhauer, Phys. Rev. Lett. **111**, 113001 (2013).
[20] D. Maxwell, D. J. Szwer, D. Paredes-Barato, H. Busche, J. D. Pritchard, A. Gauguet, K. J. Weatherill, M. P. A. Jones, and C. S. Adams, Phys. Rev. Lett. **110**, 103001 (2013).
[21] M. Fleischhauer and M. D. Lukin, Phys. Rev. Lett. **84**, 5094 (2000).
[22] W. H. Louisell, *Quantum Statistical Properties of Radiation* (Wiley, New York, 1973).
[23] A. E. Siegman, *Lasers* (University Science Books, Sausalito, 1986).
[24] M. Saffman, T. G. Walker, and K. Mølmer, Rev. Mod. Phys. **82**, 2313 (2010).
[25] M. D. Lukin, M. Fleischhauer, R. Cote, L. M. Duan, D. Jaksch, J. I. Cirac, and P. Zoller, Phys. Rev. Lett. **87**, 037901 (2001).
[26] P. Bienias, S. Choi, O. Firstenberg, M. F. Maghrebi, M. Gullans, M. D. Lukin, A. V. Gorshkov, and H. P. Büchler, Phys. Rev. A **90**, 053804 (2014).
[27] M. Moos, R. Unanyan, and M. Fleischhauer (unpublished).
[28] Note that the potentials describing scattering between different excited modes $u_{\mu\nu}$ and $u_{\mu'\nu'}$ are suppressed by at least an additional order of magnitude and decay much faster compared to the interaction between the initial Gaussian modes.
[29] H. J. Carmichael, *Statistical Methods in Quantum Optics 1* (Springer, Berlin, 1998).
[30] A. V. Gorshkov, J. Otterbach, M. Fleischhauer, T. Pohl, and M. D. Lukin, Phys. Rev. Lett. **107**, 133602 (2011).
[31] T. Giamarchi, *Quantum Physics in One Dimension* (Oxford University Press, Oxford, 2003).
[32] D. E. Chang, V. Gritsev, G. Morigi, V. Vuletić, M. D. Lukin, and E. A. Demler, Nat. Phys. **4**, 884 (2008).
[33] D. G. Angelakis, M. Huo, E. Kyoseva, and L. C. Kwek, Phys. Rev. Lett. **106**, 153601 (2011).
[34] The generalization of the Fermi energy to the bosonic system is justified since the kinetic energy per particle approaches that of free fermions for not too large a_B and Θ.
[35] H. P. Büchler, New. J. Phys. **13**, 093040 (2011).
[36] M. Dalmonte, G. Pupillo, and P. Zoller, Phys. Rev. Lett. **105**, 140401 (2010).
[37] C. Mewes and M. Fleischhauer, Phys. Rev. A **66**, 033820 (2002).
[38] M. Fleischhauer and M. D. Lukin, Phys. Rev. A **65**, 022314 (2002).
[39] L. Karpa, G. Nikoghosyan, F. Vewinger, M. Fleischhauer, and M. Weitz, Phys. Rev. Lett. **103**, 093601 (2009).
[40] G. Günter, H. Schempp, M. Robert-de-St-Vincent, V. Gavryusev, S. Helmrich, C. S. Hofmann, S. Whitlock, and M. Weidemüller, Science **342**, 954 (2013).